Journal of Medicinal Chemistry

ARTICLE

pubs.acs.org/jmc

Discovery of 2-(4-Methylfuran-2(5*H*)-ylidene)malononitrile and Thieno[3,2-*b*]thiophene-2-carboxylic Acid Derivatives as G Protein-Coupled Receptor 35 (GPR35) Agonists

Huayun Deng, Haibei Hu, Mingqian He, Jieyu Hu, Weijun Niu, Ann M. Ferrie, and Ye Fang*

Biochemical Technologies, Science and Technology Division, Corning Inc., Corning, New York 14831, United States

Supporting Information

ABSTRACT: Screening with dynamic mass redistribution (DMR) assays in a native cell line HT-29 led to identification of two novel series of chemical compounds, 2-(4-methylfuran-2(5*H*)-ylidene)malononitrile and thieno[3,2-*b*]-thiophene-2-carboxylic acid derivatives, as GPR35 agonists. Of these, 2-(3-cyano-5-(3,4-dichlorophenyl)-4,5-dimethylfuran-2(5*H*)-ylidene)malononitrile (YE120) and 6-bromo-3-methylthieno[3,2-*b*]thiophene-2-carboxylic acid (YE210) were found to be the two most potent GPR35 agonists with an EC_{50} of 32.5 ± 1.7 nM and 63.7 ± 4.1 nM, respectively. Both agonists exhibited better potency than that of zaprinast, a known GPR35 agonist. DMR antagonist assays, knockdown of GPR35 with interference RNA, receptor internalization assays, and Tango β-arrestin translocation assays confirmed that the agonist activity of these ligands is specific to GPR35. The present study provides novel chemical series as a starting point for further investigations of GPR35 biology and pharmacology.

Novel GPR35 agonists

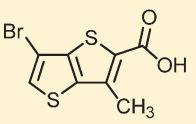

16a
EC_{50}: 64nM

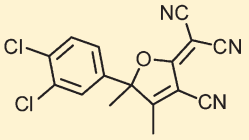

1
EC_{50}: 32nM

INTRODUCTION

G protein-coupled receptor 35 (GPR35) is an orphan G protein-coupled receptor (GPCR) and is believed to play a role in hypertension,[1] coronary artery disease,[2] asthma,[3] pain,[4,5] early onset inflammatory bowel disease,[6] and cancers.[7] Both kynurenic acid[8] and 2-acyl lysophosphatidic acid[9] have been postulated to be natural agonists for GPR35. However, there are only a handful compounds that have been reported in literature to exhibit either agonist or antagonist activity on GPR35. These compounds include zaprinast,[10] pamoic acid,[4] NPPB (5-nitro-2-(3-phenylpropylamino)-benzoate),[11] cromolyn and dicumarol,[3] luteolin, quercetin, and niflumic acid,[12] all of which are GPR35 agonists. A couple of GPR35 antagonists including compound **17** (CID-2745687, methyl-5-[(*tert*-butylcarbamothioylhydrazinylidene)-methyl]-1-(2,4-difluorophenyl)-pyrazole-4-carboxylate) have also been reported.[4] Thus, identification of novel GPR35 ligands would be beneficial to further elucidate the biology and therapeutic potentials of GPR35.

Conventional pharmacological assays often measure single signaling molecules, one at a time, downstream receptor activation and signaling. Thus, these assays often encounter difficulties to identify ligands for poorly characterized receptors such as GPR35, whose signaling pathways and biology are largely unknown. Recently, dynamic mass redistribution (DMR) assays have been emerging as a powerful tool to delineate receptor biology and drug pharmacology in native cells.[13−17] DMR assays are enabled by a label-free optical biosensor, which transforms a cellular response into an integrated and kinetic response, termed DMR.[18] Because of its pathway-unbiased yet pathway-sensitive nature in measurement, it has been hypothesized that DMR assays could offer an unprecedented advantage to discover novel ligands for receptors, particularly orphan receptors.[19] We set out to test such a hypothesis by screening an internally made chemical library against endogenous GPR35 in a native cell line, HT-29. The library consists of 660 intermediates synthesized in house, and these intermediates were originally designed for applications in nonlinear optics[20] and organic field-effect transistors.[21] The chemical library was chosen because (1) these chemicals were not designed for pharmacological applications so their pharmacological activities were unknown, and (2) some chemicals contain malononitrile group, similar to tyrphostins. Certain tyrphostin analogues have been demonstrated to be GPR35 agonists in our laboratory.[22] Using DMR assays, we had discovered two novel chemical series, 2-(4-methylfuran-2(5*H*)-ylidene)malononitrile and thieno[3,2-*b*]thiophene-2-carboxylic acid derivatives, as GPR35 agonists.

CHEMISTRY

2-(4-Methylfuran-2(5*H*)-ylidene)malononitrile compounds were synthesized via the reaction of α-ketols with 2 equiv of malononitrile under basic conditions. This reaction starts with a Knoevenagel condensation, followed by the hydroxyl group attacking one of the nitriles to form an iminolactone intermediate, which reacts again with malononitrile to result in the final products. The detailed synthesis of compounds **1** (**YE120**) and **2**−**8** have been reported previously.[20] Followed the same

Received: July 26, 2011
Published: September 27, 2011

Scheme 1

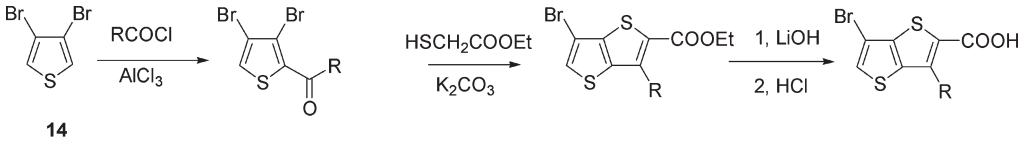

14a	R = CH_3	**15a**	R = CH_3	**16a**	R = CH_3
14b	R = C_8H_{17}	**15b**	R = C_8H_{17}	**16b**	R = C_8H_{17}
14c	R = $C_{11}H_{23}$	**15c**	R = $C_{11}H_{23}$	**16c**	R = $C_{11}H_{23}$
14d	R = $C_{13}H_{27}$	**15d**	R = $C_{13}H_{27}$	**16d**	R = $C_{13}H_{27}$
14e	R = $C_{15}H_{31}$	**15e**	R = $C_{15}H_{31}$	**16e**	R = $C_{15}H_{31}$

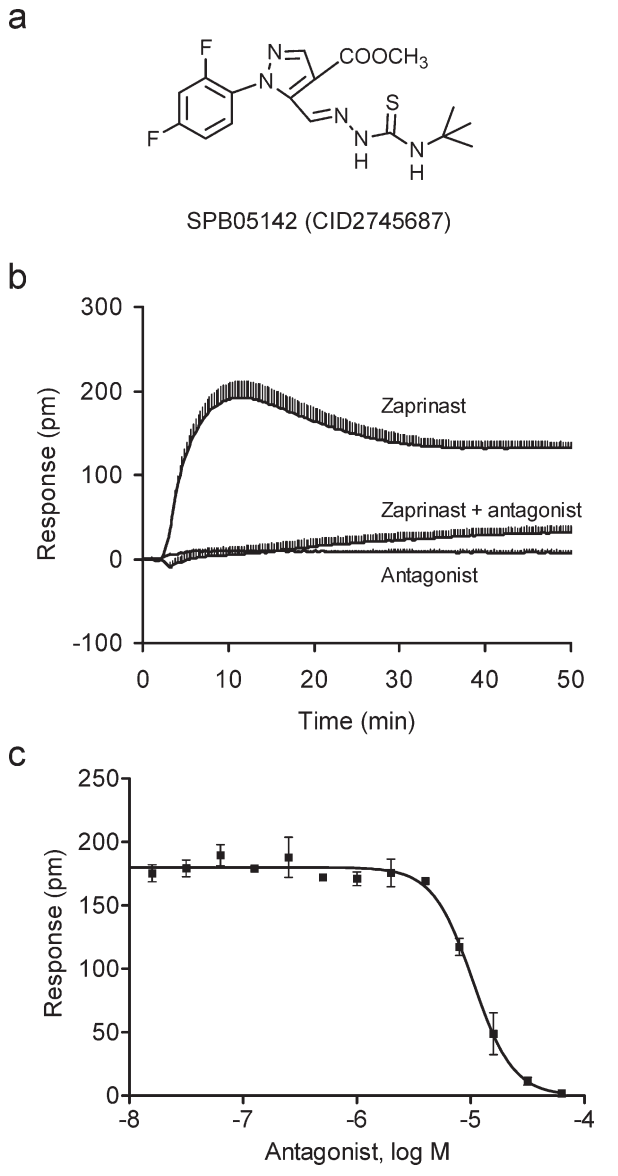

Figure 1. DMR characteristics of known GPR35 ligands in HT29. (a) Structure of a known GPR35 antagonist compound **17**. (b) The DMR arising from zaprinast (500 nM), the antagonist compound **17** (32 μM), and zaprinast (500 nM) + compound **17** (32 μM). (c) The dose-dependent blockage of the zaprinast DMR by compound **17**. The data represents mean ± sd (standard deviation) from two independent measurements, each in duplicate (n = 4).

procedure, compound **9** was prepared from 3-hydroxy-3-methylbutan-2-one.

Thieno[3,2-*b*]thiophene-2-carboxylic acid derivatives were synthesized using an aldehyde or ketone-based ring closure reaction, followed by hydrolysis.[21] Specifically, compounds **10**, **11**, **12**, and **13** were synthesized through hydrolysis of the products from a ring closure reaction of ethyl mercaptoacetate with 3-bromothiophene-2-carbaldehyde, 1-(3-bromothiophen-2-yl)heptan-1-one, 3-bromo-4-hexylthiophene-2-carbaldehyde, or 3-bromo-6-methylthieno[3,2-*b*]thiophene-2-carbaldehyde, respectively. For compounds **16a**−**e**, acyl-substituted 3,4-dibromothiophene **14a**−**e** was first synthesized through a Friedel−Crafts acylation of 3,4-dibromothiophene (**14**) with acyl chloride. The ketone **14a**−**e** then underwent a ring closure reaction with ethyl mercaptoacetate, leading to ethyl 3-alkyl-6-bromothieno[3,2-*b*]thiophene-2-carboxylate **15a**−**e**. After hydrolysis, compounds **16a**−**e** was obtained (Scheme 1). Purity of all the final compounds was found to be greater than 95%, as measured by reverse phase HPLC on a C_{18} column.

RESULTS AND DISCUSSION

Screening GPR35 Agonists with DMR Assays. Because human colorectal adenocarcinoma cell line HT29 endogenously expresses functional GPR35,[22] this cell line was chosen to screen GPR35 agonists. The known GPR35 agonist zaprinast was used as a reference agonist. Previously, we have showed that zaprinast resulted in a robust DMR with an EC_{50} of 0.16 ± 0.02 μM and internalization of GPR35 in HT29.[22] Compound **17**, a known GPR35 antagonist, did not lead to any detectable DMR in HT29, but dose-dependently blocked the zaprinast DMR with an IC_{50} of 10.5 ± 0.3 μM (n = 4) (Figure1). At the highest dose (64 μM), compound **17** almost completely blocked the zaprinast DMR. These results suggest that the zaprinast-induced DMR in HT29 is specific to the activation of GPR35.

To screen ligands for GPR35, we used a two-step DMR desensitization assay. This assay begins with DMR agonist assay to examine all compounds for their agonist activity in HT29, followed by DMR desensitization assay to determine the ability of each compound to block or desensitize the cells responding to the repeated stimulation with zaprinast at a saturating dose (1 μM). Both agonist and desensitization assays were monitored in real time for 1 h using Epic system. The Epic system is a label-free optical biosensor microtiter plate reader tailored to 384-well resonant waveguide grating biosensor plates. A cellular response was recorded as a shift in resonant wavelength in picometer (pm). The adoption of such a two-step sequential assay format is based on that (1) DMR assays are noninvasive, thus enabling

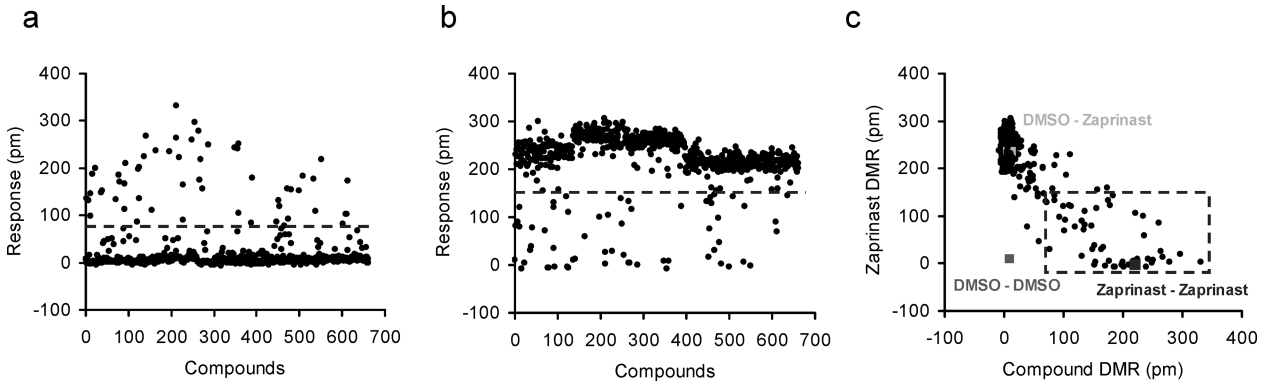

Figure 2. Screening GPR35 agonists. (a) The DMR amplitudes of compounds in the library as a function of compounds. (b) The DMR signals induced by zaprinast after the cells were prestimulated with compounds in the library. (c) The correlation between the compound DMR in native cells and the zaprinast DMR in the compound-pretreated cells.

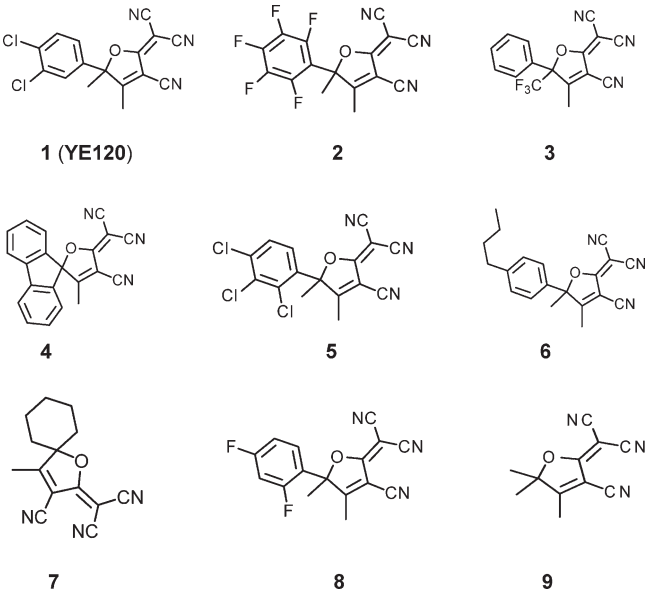

Figure 3. Structures of 2-(4-methylfuran-2(5*H*)-ylidene)malononitrile derivatives identified as GPR35 agonists.

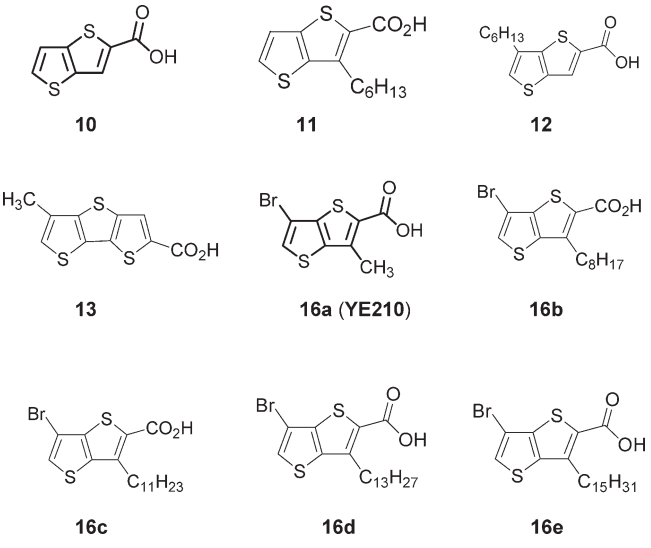

Figure 4. Structures of thieno[3,2-*b*]thiophene-2-carboxylic acid derivatives identified as GPR35 agonists.

multiple step assays, and (2) the cells pretreated with an agonist become desensitized to the repeated stimulation with a second agonist when two agonists activate the same receptor.[23] Such a homologous desensitization is common to almost all GPCR signaling. The real-time kinetic responses of all compounds were collected and analyzed.

To identify hits, the amplitudes at 8 min poststimulation of all compound-induced responses were determined and used as a basis for hit identification in the agonist screen. This is because zaprinast at a saturating dose (1 μM) led to a maximal response peaked at about 8 min poststimulation (246 $\pm$ 11 pm, n = 32). Using the compound DMR amplitudes greater than 30% of the zaprinast response as the hit identification criteria, 55 hits in total were identified (Figure2a).

For the desensitization screen, the amplitudes of the zaprinast DMR during the desensitization step were determined for each compound. As a positive control, zaprinast in the dimethyl sulfoxide (DMSO) treated cells gave rise to a DMR with an amplitude of 238 $\pm$ 25 pm (n = 90). Using 3$\times$ σ of the positive control as a basis for hit selection, we found 65 hits that led to a zaprinast DMR smaller than 160 pm (Figure2b). The correlation analysis suggests that 53 hits were common between the two assays (Figure2c).

Structure and activity analysis led to identification of 20 compounds that belong to two chemical series, 2-(4-methylfuran-2(5*H*)-ylidene)malononitrile and thieno[3,2-*b*]thiophene-2-carboxylic acid derivatives. Eighteen of these compounds were further characterized in detail (Figures 3 and 4), given that there were sufficient amounts available for follow-up studies. The remaining 33 compounds were either orphan in structure or contain aldehyde or ketone groups, thus excluded in further studies.

The Agonist Specificity of Compounds to GPR35. Given that many compounds may exhibit polypharmacology and DMR measurement is integrative in nature, a compound-induced DMR may contain contributions from multiple targets/pathways with which the compound intervene. Thus, we first examined the specificity of the 18 compound-induced DMR using DMR antagonist assays. Each compound was assayed at a dose close to its respective EC_{80} or EC_{100} in the presence of compound **17**.

dx.doi.org/10.1021/jm200999f |*J. Med. Chem.* 2011, 54, 7385–7396

Table 1. Compounds, Their Efficacy in DMR Assays or Tango Assays Relative to Zaprinast, and Potency (EC_{50} to Trigger DMR, IC_{50} to Desensitize Cells upon Repeated Stimulation with 1 μM Zaprinast, IC_{50} of the Known GPR35 Antagonist Compound 17 to Block the Agonist-Induced DMR, and EC_{50} to Trigger β-Arrestin Translocation in Tango Assays)

	DMR assays				Tango assays	
compd	% zaprinast	EC_{50} (μM)	desensitization IC_{50} (μM)	Antagonist IC_{50} (μM)	% zaprinast	EC_{50} (μM)
zaprinast	100 ± 5	0.16 ± 0.02	1.22 ± 0.10	10.5 ± 0.3	100 ± 7	4.20 ± 0.25
1	97 ± 6	0.032 ± 0.002	0.060 ± 0.007	12.8 ± 0.8	29 ± 5	10.2 ± 0.91
2	84 ± 9	3.35 ± 0.25	4.48 ± 0.36	14.7 ± 1.2	inactive	inactive
3	99 ± 4	3.50 ± 0.21	1.94 ± 0.23	20.9 ± 1.5	14 ± 5	>50
4	90 ± 6	6.6 ± 0.5	21.6 ± 3.1	5.1 ± 0.7	ND	ND
5	90 ± 5	11.1 ± 1.7	10.3 ± 0.9	11.4 ± 1.3	ND	ND
6	100 ± 4	15.3 ± 2.1	6.4 ± 1.1	13.3 ± 0.9	inactive	inactive
7	106 ± 9	45.9 ± 4.9	16.4 ± 1.5	22.8 ± 1.7	weak	>50
8	99 ± 7	53.9 ± 5.4	48.9 ± 3.7	8.2 ± 1.1	inactive	inactive
9	87 ± 5	17.1 ± 2.2	12.1 ± 1.6	7.9 ± 0.5	weak	>50
10	81 ± 4	42.4 ± 3.7	57.0 ± 4.1	6.3 ± 0.6	inactive	inactive
11	99 ± 4	3.44 ± 0.17	1.49 ± 0.12	27.6 ± 3.5	20 ± 4	>50
12	103 ± 3	9.4 ± 0.7	4.69 ± 0.09	16.0 ± 2.1	9 ± 3	>50
13	118 ± 3	6.0 ± 1.2	6.07 ± 0.14	18.2 ± 1.7	19 ± 4	>50
16a	105 ± 3	0.064 ± 0.004	0.11 ± 0.01	6.9 ± 0.5	104 ± 5	15.0 ± 1.2
16b	103 ± 7	1.46 ± 0.17	1.05 ± 0.07	25.8 ± 1.9	8 ± 3	>50
16c	87 ± 9	1.89 ± 0.23	0.57 ± 0.05	23.8 ± 2.4	55 ± 6	22.7 ± 3.1
16d	77 ± 7	2.31 ± 0.35	1.87 ± 0.14	24.8 ± 1.5	inactive	inactive
16e	81 ± 11	4.56 ± 0.41	5.92 ± 0.67	20.2 ± 1.4	inactive	inactive
15a	inactive	NA	NA	NA	inactive	inactive

Results showed that compound **17** dose-dependently attenuated the DMR arising from all 18 compounds with similar potency (Table 1). However, compound **17** at 64 μM blocked the DMR induced by most compounds, except for compounds **5**, **7**, **8**, **11**, and **13**, whose DMR were only partially suppressed (Figures 5 and 6). Together with the observed ability of these compounds to desensitize the cells to the zaprinast stimulation, these results suggest that the DMR induced by these compounds are mostly specific to GPR35, although we can not rule out the possibility of compounds **5**, **7**, **8**, **11**, and **13** to activate endogenous target(s) besides GPR35.

We further examined the specificity of these ligands using DMR agonist assays after interference RNA (RNAi) knockdown of GPR35. Results showed that knockdown of GPR35 using short hairpin RNA (shRNA) significantly suppressed the DMR signals induced by the five compounds examined (Figure.7a−e). Western blot confirmed the efficiency of ShRNA knockdown at least by 60% (Figure 7f). Noticeably, distinct compounds gave rise to different sensitivity to RNAi knockdown. This may be due to the difference in efficacy of these compounds. It is known that partial agonists are generally more sensitive to the reduction of functional receptors than full agonists.[24,25]

Next, we examined the ability of representative compounds to cause receptor internalization, a hallmark of the activation of most GPCRs. We specifically compared compound **16a** with its analogue, compound **15a** (Figure 8a). Unlike **16a**, **15a** was found to be inactive in DMR assays (Figure 8b). To study agonist-induced internalization of endogenous GPR35, the cells were first exposed to an agonist at a given dose for 1 h at 37 °C. After fixation and permeabilization, the cells were incubated with an anti-GPR35 antibody (T-14, intracellular domain), followed by staining with a fluorescently labeled secondary antibody. Fluorescent confocal imaging showed that GPR35 in the unstimulated cells was primarily located at the cell surface (Figure 8c), and stimulation with **16a** caused significant internalization of GPR35 (Figure 8d). As expected, **15a** was inactive in the receptor internalization assay (Figure 8e).

Last, we examined the ability of these compounds to cause β-arrestin translocation using the Tango GPR35 arrestin assays. This assay uses Tango GPR35-*bla* U2OS cells to detect GPR35 agonist-induced recruitment of TEV protease tagged β-arrestin molecules to the GPR35-Gal4-VP16 transcription factor fusion protein linked by a TEV protease cleavage site. The β-arrestin recruitment leads to release of the transcription factor from the C-terminus of GPR35, which, in turn, translocates to the nucleus and activates the expression of β-lactamase. The activity of β-lactamase is then assayed with the cell permeable LiveBLAzer fluorescence resonance energy transfer (FRET) B/G substrate. Results showed that zaprinast led to a dose-dependent response in Tango GPR35-*bla* U2OS cells with a significantly right-shifted potency, EC_{50} of 4.20 ± 0.25 μM (n = 4) (Figure9; Table 1). Among all the compounds examined, compound **1**, **3**, **16a**, and **16c** gave rise to dose-dependent and saturable responses but with distinct potency and efficacy (Figure 9; Table 1). Compounds **7**, **9**, **10**, **11**, **12**, **13**, and **16b** also led to detectable responses (Figure9 and Table 1). However, **2**, **4**, **5**, **6**, **8**, **15a**, **16d**, and **16e** all at a dose up to 128 μM were inactive in this assay. These results suggest that **16a** is a full agonist in the arrestin translocation assay, while **1**, **3**, **7**, **9**, **10**, **11**, **12**, **13**, **16b**, and **16c** are partial agonists. However, considering the common right-shifted potency of GPR35 agonists obtained using the Tango assay, we can not rule out the possibility that the other compounds may also be active but with much lower potency. Collectively, we

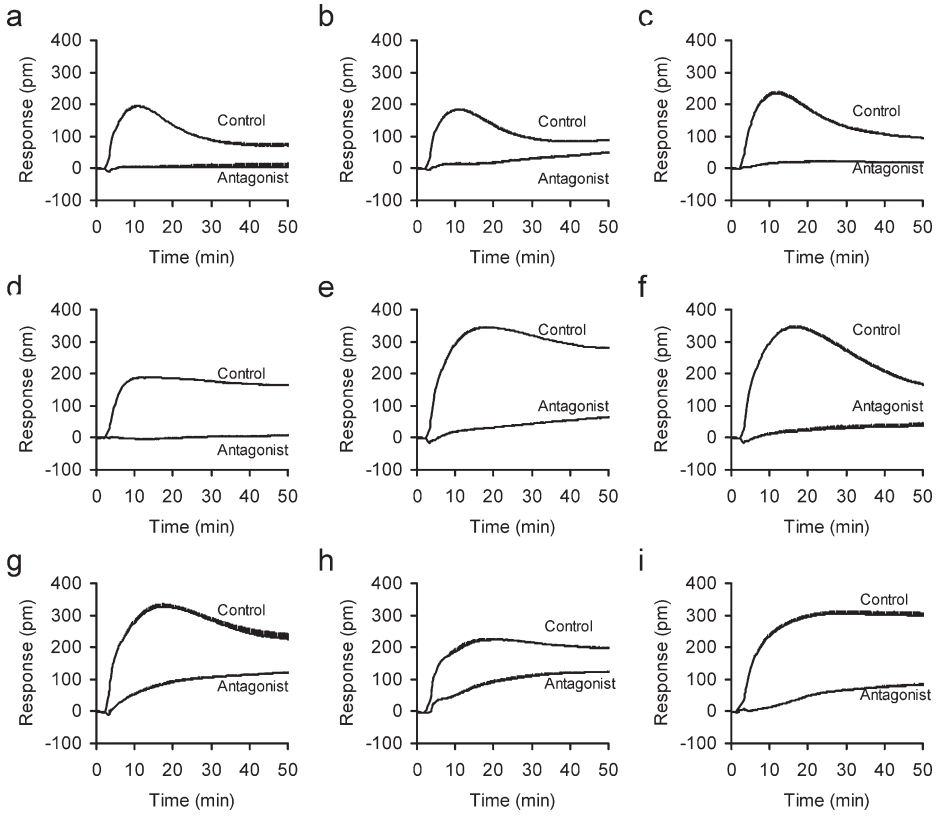

Figure 5. The DMR characteristics of 2-(4-methylfuran-2(5*H*)-ylidene)malononitrile derivatives. (a−i) Compound **1** (250 nM), **2** (8 μM), **3** (4 μM), **4** (8 μM), **5** (16 μM), **6** (16 μM), 7 (32 μM), **8** (32 μM), and **9** (32 μM), respectively. Each compound-induced DMR (Control) was compared to its corresponding DMR in the presence of 32 μM **17**, the known GPR35 antagonist (Antagonist). The data represents mean ± sd from two independent measurements, each with four replicates (n = 8).

demonstrated that the two chemical series compounds are GPR35 agonists.

Structure and Activity Analysis. To further examine structure and activity analysis, we determined the potency of all 18 compounds to trigger DMR signals in HT29 cells using DMR assays. The results showed that all compounds gave rise to a clear dose-dependent response (Figure10). All compounds led to a saturable response at the dose ranges examined. However, there are significant differences in potency, efficacy, and DMR characteristics of these compounds (Table 1, Figures 5 and 6).

The DMR desensitization assays showed that all compounds also dose-dependently desensitized the cells to the repeated stimulation with 1 μM zaprinast, and the rank order of their apparent IC_{50} values to desensitize the cells is similar to that of their respective EC_{50} values (Figure11). This suggests that all compounds activate GPR35 as zaprinast does. Of these, 2-(3-cyano-5-(3,4-dichlorophenyl)-4,5-dimethylfuran-2(5*H*)-ylidene)malononitrile (**1**, **YE120**) and 6-bromo-3-methylthieno[3,2-*b*]-thiophene-2-carboxylic acid (**16a**, **YE210**)[26] were the two most potent agonists, and their respective EC_{50} was 32.5 ± 1.7 nM (n = 4) and 63.7 ± 4.1 nM (n = 4), both of which are more potent than zaprinast (163 ± 19 nM, n = 4).

With the identification of potent compound **16a**, we further examined the functional groups critical to its agonist activity. Changing the carboxylic acid to an ethyl carboxylate led to compound **15a** (Figure 8a). Compound **15a** was found to be inactive in HT-29 in DMR agonist assay (Figure 8b) and also unable to trigger receptor internalization (Figure 8e). Removal of the bromo group at C6 and replacing the methyl group with hexyl group led to compound **11**, which exhibited about 54-fold decrease in potency (Table 1). Removal of both bromo and methyl groups resulted in compound **10**, which decreased its potency by over 600-fold (Table 1). Replacing the methyl group with a long-chained *n*-alkyl group resulted in compound **16b**−**e** and also reduced both potency and efficacy. Further, converting the backbone from thieno[3,2-*b*]thiophene into dithieno-[3,2-*b*:2′,3′-*d*]thiophene led to compound **13**, which also exhibited a lower potency. These results clearly reveal the importance of 3- and 6-position groups, carboxylic acid, and the size of backbone for its potency and agonist activity of thieno[3,2-*b*]thiophene-2-carboxylic acid derivatives. Compound **16a** is a full agonist in both DMR and Tango assays, while **11**, **12**, **13**, **16b**, and **16c** are partial agonists in Tango assays.

Next, we examined the structure and activity relationship of 2-(4-methylfuran-2(5*H*)-ylidene)malononitrile derivatives for their agonist activity. Adding a chloro group at the 2-position of the phenyl group of compound **1** leads to **5**, which exhibited 350-fold decrease in potency to trigger DMR signal and became inactive in Tango assay. Replacing 3,4-dichlorophenyl group with pentafluorophenyl group (**2**) or 2,4-bifluorophenyl group (**8**) or 4′-*n*-butylphenyl group (**6**) or methyl group (**9**) all led to significant lost in its potency to trigger DMR as well as its efficacy to trigger β-arrestin translocation. Replacing 3,4-dichlorophenyl and methyl groups at the 5-position of its furan ring with phenyl and spiro groups leads to compound **3**, which exhibited lower potency in both DMR and Tango assays. These results suggest

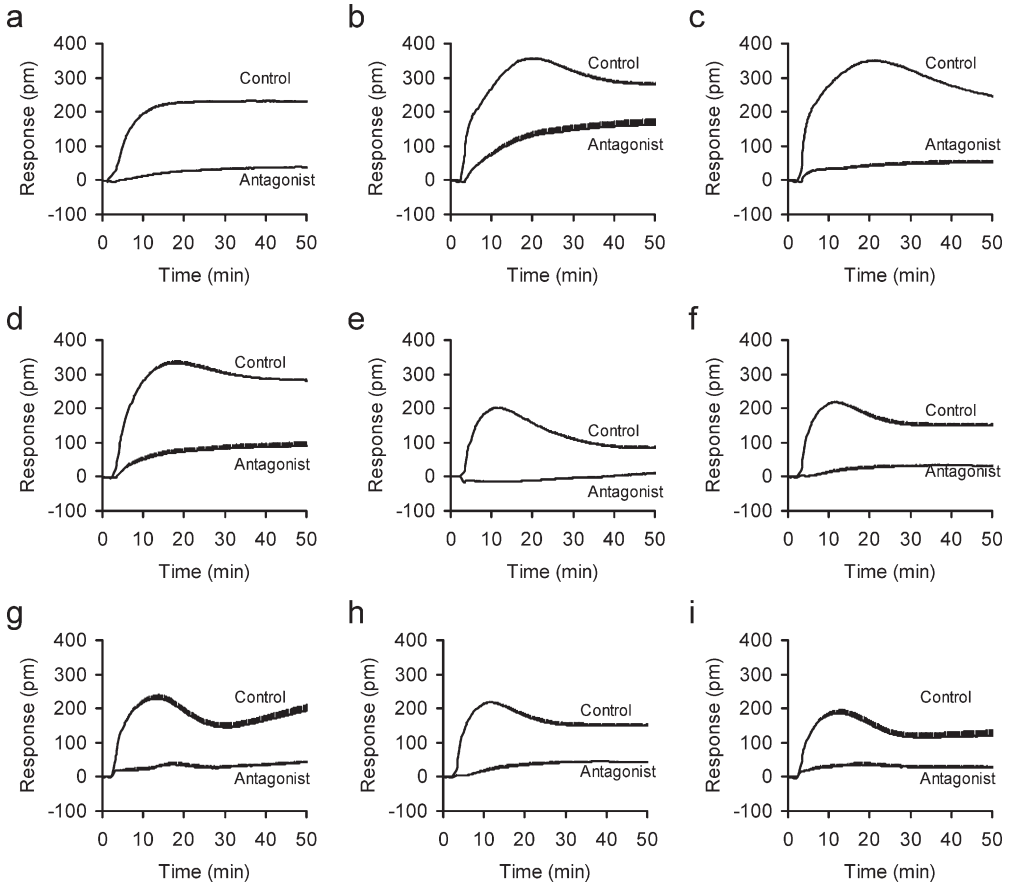

Figure 6. The DMR characteristics of thieno[3,2-*b*]thiophene-2-carboxylic acid derivatives. (a–i) Compound **10** (32 μM), **11** (16 μM), **12** (16 μM), **13** (16 μM), **16a** (250 nM), **16b** (8 μM), **16c** (8 μM), **16d** (8 μM), and **16e** (8 μM), respectively. Each compound induced DMR (Control) was compared to its corresponding DMR in the presence of 32 μM compound **17**, the known GPR35 antagonist (Antagonist). The data represents mean ± sd from two independent measurements, each with four replicates (n = 8).

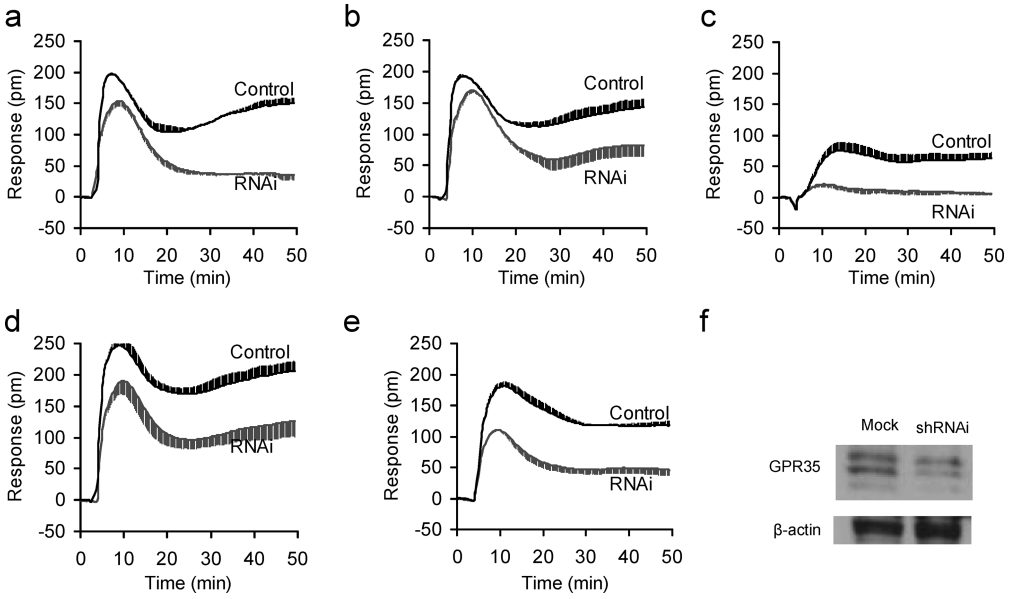

Figure 7. shRNA knockdown of GPR35 significantly attenuated the DMR induced by GPR35 agonists identified. (a) Zaprinast, (b) **1**, (c) **9**, (d) **16a**, and (e) **13**. All compounds were assayed at 10 μM. The data represents mean ± sd from four replicates (n = 4) for all compounds. The mock transfection was used the positive control. (f) Western blotting showed the knockdown of GPR35 proteins by the shRNA.

dx.doi.org/10.1021/jm200999f |*J. Med. Chem.* 2011, 54, 7385–7396

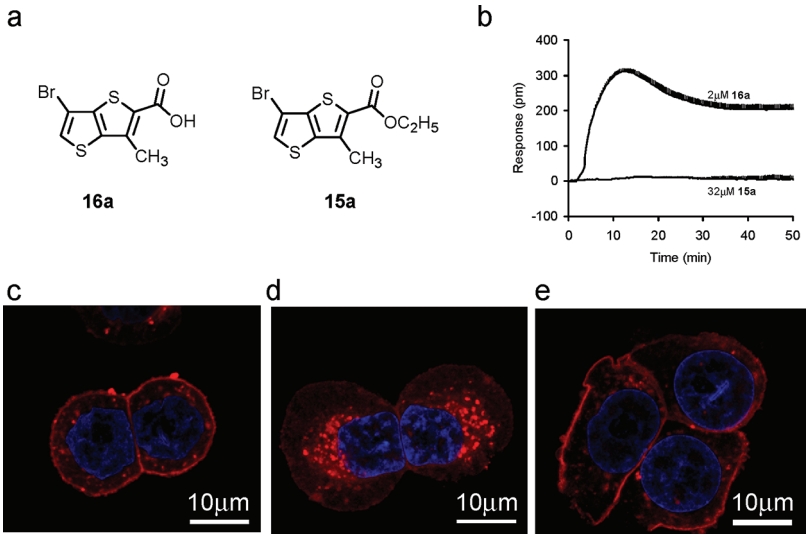

Figure 8. Compound **15a** was unable to activate GPR35. (a) Structures of **15a** and **16a**. (b) The net-zero DMR induced by **15a**, in comparison with that by **16a**. The data represents mean ± sd from four replicates (n = 4). (c–e) Representative fluorescence images of HT-29 under different conditions: unstimulated (c), stimulated with 1 μM **16a** (d), or stimulated with 10 μM compound **15a** (e). The images were obtained after compound treatment for 1 h, permeabilized, and stained with anti-GPR35, followed by fluorescent secondary antibody. Red: GPR35 stains. Blue: nuclei stains with DAPI.

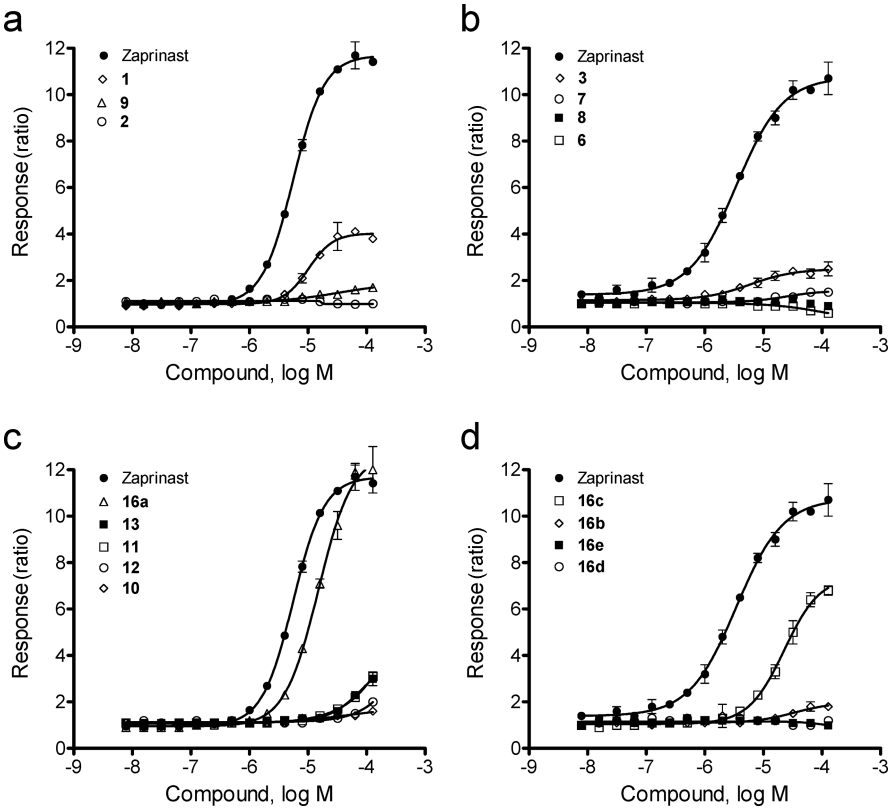

Figure 9. Dose-dependent responses of GPR35 ligands as measured using Tango β-arrestin translocation gene reporter assays. The coumarin to fluorescein ratio was plotted as a function of ligand doses. Zaprinast was included as a positive control. The data represents mean ± sd from two independent measurements, each in duplicate (n = 4).

that the functional groups at the 5-position of its furan ring is critical to the agonist activity of compound **1**.

Finally, we examined the ligand-directed functional selectivity of GPR35 agonists. The known GPR35 agonist zaprinast were found to be active in both DMR and Tango assays, with an EC_{50} of 0.16 and 1.47 μM, respectively. Compared to zaprinast, both **1** and **16a** are more potent to trigger DMR signal (EC_{50} of 0.032 and 0.064 μM, respectively) but less potent to result in β-arrestin

dx.doi.org/10.1021/jm200999f |J. Med. Chem. 2011, 54, 7385–7396

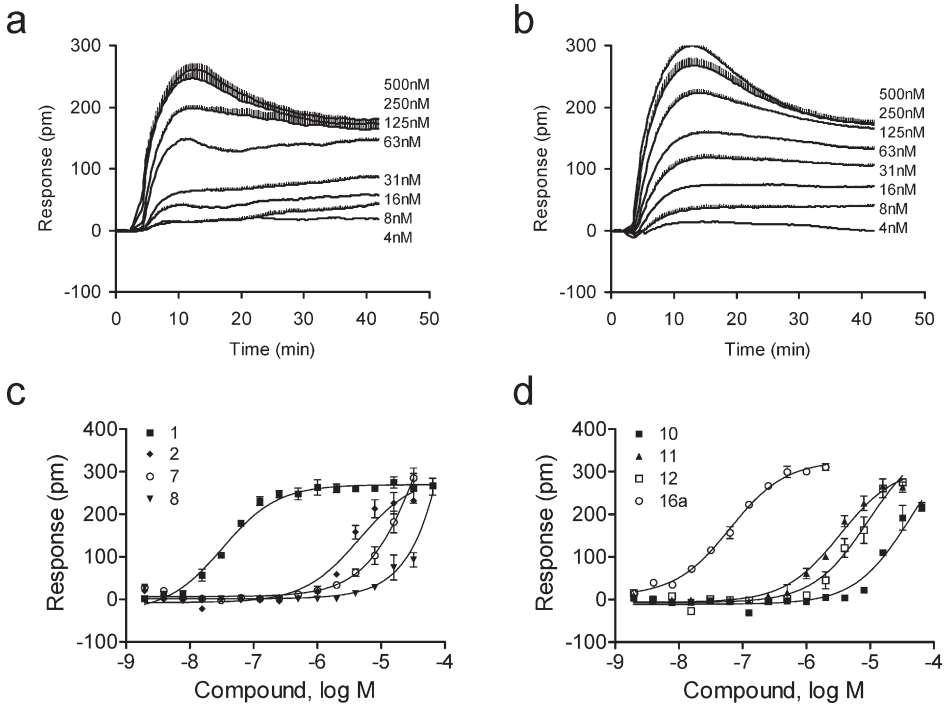

Figure 10. Representative DMR signals of GPR35 agonists identified. (a) The dose-dependent DMR induced by **1**, (b) the dose-dependent DMR induced by **16a**, (c) the amplitudes of the DMR induced by 2-(4-methylfuran-2(5*H*)-ylidene)malononitrile derivatives as a function of doses, and (d) the amplitudes of the DMR induced by thieno[3,2-*b*]thiophene-2-carboxylic acid derivatives as a function of doses.

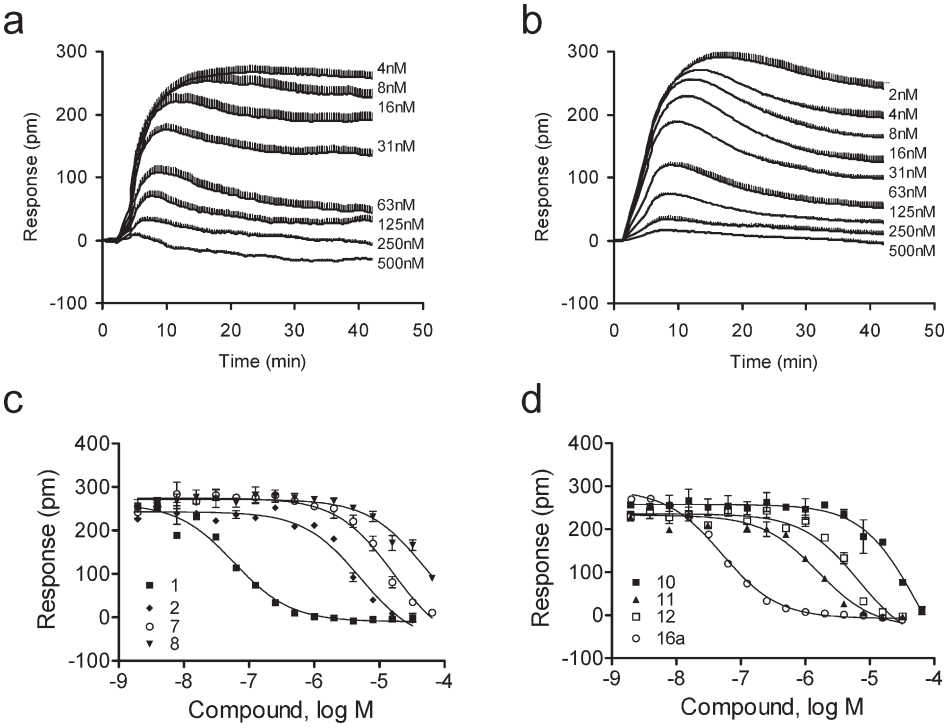

Figure 11. The dose-dependent desensitization by GPR35 agonists identified to the repeated stimulation with zaprinast (1 μM). (a,b) Real-time zaprinast DMR after pretreatment with **1** (a) and **2** (b), respectively, and (c) and (d) dose-dependent desensitization by thieno[3,2-*b*]thiophene-2-carboxylic acid derivatives (c) and thieno[3,2-*b*]thiophene-2-carboxylic acid derivatives (d), respectively.

translocation (EC_{50} of 10.2 and 15.0 μM, respectively). Further, compared to zaprinast, **16a** is also a full agonist in both DMR and Tango assays, but **1** is only a full agonist to trigger DMR but a partial agonist to result in β-arrestin translocation. Such an assay

dx.doi.org/10.1021/jm200999f |*J. Med. Chem.* 2011, 54, 7385–7396

readout-dependent potency and efficacy suggests that different GPR35 agonists display ligand-directed functional selectivity.[27]

CONCLUSIONS

We have screened an internally made compound library against a poorly characterized orphan receptor GPR35 using DMR assays and have identified two chemical series, 2-(4-methylfuran-2(5*H*)-ylidene)malononitrile and thieno[3,2-*b*]thiophene-2-carboxylic acid derivatives, which represent novel classes of GPR35 agonists. The agonist activity of 18 compounds was found to be specific to GPR35 based on DMR antagonist assays using a known GPR35 antagonist compound **17**, DMR desensitization assays against zaprinast, receptor internalization, and β-arrestin translocation assays. The structure−activity relationships of these ligands as GPR35 agonists have been also explored. Notably, the carboxylic acid group of thieno[3,2-*b*]thiophene-2-carboxylic acid derivatives was found to be critical to activate GPR35. Because malononitrile is relatively acidic under physiological conditions, it may also be important to the agonist activity of 2-(4-methylfuran-2(5*H*)-ylidene)malononitrile derivatives. This study expands current pharmacological tools to characterize the biology and functions of GPR35 and presents a good starting point to design and optimize new GPR35 ligands.

EXPERIMENTAL SECTION

Chemistry. All reactions were performed in reagent grade solvent. The progress of the reactions was checked by GC/MS (Agilent 7820A GC/5875 MS) and analytical thin-layer chromatography (TLC). Plates were visualized first with UV illumination, followed by charring with phosphomolybdic acid. Flash column chromatography was performed using silica gel (200−300 mesh). ^{1}H NMR spectra were recorded by Bruker-300 MHz NMR spectrometers in the indicated deuterated solvents and are reported in parts per million (ppm) on the δ scale relative to residual CD_2Cl_2 (δ 5.32), THF-D7H (δ 3.58, 1.73), and acetone-d_6 (δ 2.05). Splitting patterns are provided as apparent multiplicities: s (singlet), d (doublet), t (triplet), m (multiplet), and br (broad). ^{13}C NMR spectra were recorded in the indicated deuterated solvents by Bruker-75 MHz and are reported in parts per million (ppm) on the δ scale relative to residual CD_2Cl_2 (δ 53.8) and DMSO-d_6 (δ 39.5). High-resolution mass spectra (HRMS) were recorded on an Agilent 1100 mass spectrometer using Matrix-assisted laser desorption ionization (MALDI) or electron ionization (EI). We chose the negative ion mode of operation for EI mass spectroscopy characterization of fused thiophene molecules containing an acidic side group, which resulted in the generation of the deprotonated molecular ion from these molecules. The purity determination of all reported compounds was performed with an Agilent 1100 equipped with Waters columns (Atlantis T3, 2.1 mm × 50 mm, 3 μm; or Atlantis dC18, 2.1 mm × 50 mm, 5 μm) eluted for >10 min with a gradient mixture of H_2O−acetonitrile with formic or trifluoroacetic acid at wavelengths of 220, 254, and 280 nm. All compounds analyzed were >95% pure. Synthesis and characterization of compound **1** (2-(3-cyano-5-(3,4-dichlorophenyl)-4,5-dimethylfuran-2(5*H*)-ylidene)malononitrile, **2** 2-(3-cyano-4,5-dimethyl-5-(perfluorophenyl)furan-2(5*H*)-ylidene)malononitrile), **3** (2-(3-cyano-4-methyl-5-phenyl-5-(trifluoromethyl)furan-2(5*H*)-ylidene)malononitrile), **4** (2-(4′-cyano-3′-methyl-5′*H*-spiro-[fluorene-9,2′-furan]-5′-ylidene)malononitrile), **5** (2-(3-cyano-4,5-dimethyl-5-(2,3,4-trichlorophenyl)furan-2(5*H*)-ylidene)malononitrile), **6** (2-(5-(4-butylphenyl)-3-cyano-4,5-dimethylfuran-2(5*H*)-ylidene)malononitrile), **7** (2-(3-cyano-4-methyl-1-oxaspiro[4.5]dec-3-en-2-ylidene)-malononitrile), and **8** (2-(3-cyano-5-(2,4-difluorophenyl)-4,5-dimethylfuran-2(5*H*)-ylidene)malononitrile) were reported previously.[20] NMR and mass spectra of other compounds were included in Supporting Information.

*2-(3-Cyano-4,5,5-trimethylfuran-2(5H)-ylidene)malononitrile (**9**).* 3-Hydroxy-3-methylbutan-2-one (1.0 equiv), malononitrile (3.2 equiv), and magnesium ethoxide (0.01 equiv) in ethanol were mixed and refluxed overnight. The solution was concentrated by removing the majority of the THF on a rotary evaporator under aspirator vacuum. The remaining residue was taken up in methylene chloride and washed with brine (2 times) and then DI water (2 times). The organic layer was dried over anhydrous $MgSO_4$ and filtered and the solvent removed. The crude product was recrystallized from denatured alcohol to afford **9**. Yield: 29%. ^{1}H NMR (300 MHz, acetone-d_6): δ 2.36 (s, 3H), 1.63 (s, 6H). HRMS (EI) for $C_{11}H_9N_3O$: calcd, 199.07; found, 199.07 [M].

*Thieno[3,2-b]thiophene-2-carboxylic Acid (**10**).* 3-Bromothiophene-2-carbaldehyde (1.0 equiv) was mixed with K_2CO_3 (4.0 equiv) in dimethylformamide (DMF) in a three-neck flask equipped with a condenser and addition funnel. After ethyl mercaptoacetate (1.0 equiv) was added dropwise at 60−70 °C, the mixture was heated overnight until no starting materials were detected by GC/MS. The mixture then was poured into water and the product was extracted by diethyl ether. The organic phase was washed with brine and dried over anhydrous $MgSO_4$. The resultant brownish crude ethyl thieno[3,2-*b*]thiophene-2-carboxylate was obtained and found to be pure enough for the next reaction. After dissolved in a mixture of THF and methanol (1:1) in the presence of 1 M LiOH and refluxed overnight, the mixture was poured into concentrated hydrochloric acid. The acid mixture was then diluted with water. Solid was filtrated, washed with water and methanol, and purified with flash column chromatography to provide the light-yellow solid of compound **10** (89% overall yield). ^{1}H NMR (300 MHz, acetone-d_6): δ 8.12 (s, 1H), 7.88 (d, 1H), 7.48 (d, 1H). HRMS (EI) for $C_7H_4O_2S_2$: calcd, 183.96; found, 138.97 [M − COOH].

*3-Hexylthieno[3,2-b]thiophene-2-carboxylic Acid (**11**).* 1-(3-Bromothiophen-2-yl)heptan-1-one (1.0 equiv) was mixed with K_2CO_3 (4.0 equiv) in DMF in a three-neck flask equipped with a condenser and addition funnel. After ethyl mercaptoacetate (1.0 equiv) was added dropwise at 60−70 °C, the mixture was heated at 60−70 °C overnight until no starting materials was detected by GC/MS. The mixture was then poured into water and extracted by diethyl ether. The organic phase was washed with brine and dried over anhydrous $MgSO_4$. The residue was the brownish crude ethyl 3-hexylthieno[3,2-*b*]thiophene-2-carboxylate, which was directly dissolved into a mixture of THF and methanol containing 1 M LiOH and refluxed overnight. The mixture was poured into concentrated hydrochloric acid. The acid mixture was then diluted with water. Solid was filtrated, washed with water and then methanol, and purified by flash column chromatograph to provide the light-yellow solid of compound **11** (83% overall yield). ^{1}H NMR (300 MHz, TDF): δ 11.48 (br, 1H), 7.68 (d, 1H), 7.31 (d, 1H), 3.19 (t, 2H), 1.42−1.31 (m, 8H), 0.89 (t, 3H). The small peaks at 3.73 (s), and 2.80 (t) indicated that compound **11** was contaminated with 3−6% byproduct. ^{13}C NMR (75 MHz, CD_2Cl_2): 145.6, 142.4, 132.3, 126.9, 120.5, 32.0, 29.9, 29.7, 23.0, 14.2. HRMS (EI) for $C_{13}H_{16}O_2S_2$: calcd, 268.06; found, 267.13 [M − H].

*6-Hexylthieno[3,2-b]thiophene-2-carboxylic Acid (**12**).* 3-Bromo-4-hexylthiophene-2-carbaldehyde (1.0 equiv) was mixed with K_2CO_3 (1.5 equiv) in DMF in a three-neck flask equipped with a condenser and an addition funnel. After ethyl mercaptoacetate (0.5 equiv) was added dropwise at room temperature, the mixture was stirred at room temperature overnight until no starting materials were detected by GC/MS. The mixture was then poured into water and extracted by ethyl acetate. Organic extracts were washed by brine and dried over $MgSO_4$ to yield the brownish crude ethyl 6-hexylthieno[3,2-*b*]thiophene-2-carboxylate, which was then dissolved into a mixture of THF and 1 M LiOH. This mixture was refluxed overnight and poured into concentrated

hydrochloric acid. The acid mixture was then diluted with water. Solid was filtrated and washed with water. The residue was recrystallized from hexane to provide the light-yellow solid of **12** (46% overall yield). ^{1}H NMR (300 MHz, CD_2Cl_2): δ 8.10 (s, 1H), 7.50 (s, 1H), 2.78 (t, 2H), 1.72−1.68 (m, 2H), 1.42−1.36 (m, 6H), 0.88 (t, 3H). HRMS (EI) for $C_{13}H_{16}O_2S_2$: calcd, 268.06; found, 267.13 [M − H].

*5-Methyldithieno[3,2-b:2′,3′-d]thiophene-2-carboxylic Acid (**13**).* 3-Bromo-6-methylthieno[3,2-*b*]thiophene-2-carbaldehyde (1.0 equiv) was reacted with ethyl mercaptoacetate (1.0 equiv) in the presence of K_2CO_3 (4.0 equiv) in DMF to provide the yellow solid ethyl 5-methyldithieno-[3,2-*b*:2′,3′-*d*]thiophene-2-carboxylate, which was then (0.16 mol) dissolved in LiOH (10% in water), THF, and methanol (2:6:1). The mixture was refluxed overnight and poured into concentrated hydrochloric acid. The residue was purified by flash column chromatography to provide the light-yellow powder **13** (73% overall yield); mp 289−290 °C. ^{1}H NMR (300 MHz, DMSO-d_6): δ 8.19 (s, 1H), 7.49 (s, 1H), 2.55 (s, 3H). ^{1}H NMR (300 MHz, TDF): δ 8.04 (s, 1H), 7.25 (s, 1H), 2.37 (s, 3H). ^{13}C NMR (75 MHz, DMSO-d_6): 163.1, 145.3, 140.0, 135.2, 134.1, 130.5, 129.2, 14.1. HRMS (EI) for $C_{10}H_6O_2S_3$: calcd, 253.95; found, 253.04 [M − H].

*General Procedure for the Synthesis of 3-Alkyl-thieno[3,2-b]thiophene-2-carboxylic Acid (**16a**−**e**).* These compounds were synthesized using the protocol shown in Scheme 1.

To a mixture of 3,4-dibromothiophene **14** (1.0 equiv) and $AlCl_3$ (2.0 equiv) in CH_2Cl_2 at 0 °C, acetyl chloride (1.0 equiv) was added dropwise under a nitrogen stream. This mixture was stirred for 2−3 h until no starting materials could be detected by GC/MS. The mixture was then poured into 6 M HCl and the organic was extracted with CH_2Cl_2 and dried over anhydrous $MgSO_4$. The mixture was then poured into 6 M HCl and the organic was extracted with CH_2Cl_2 and dried over anhydrous $MgSO_4$. Evaporation of the solvent gave the crude acetyl-substituted 3,4-dibromothiophene **14a**−**e**.

The crude acetyl-substituted 3,4-dibromothiophene (**14a**−**e**) (1.0 equiv) was mixed with K_2CO_3 (5.0 equiv) and DMF in a three-neck flask equipped with a condenser and addition funnel. After ethyl mercaptoacetate (1.0 equiv) was added dropwise at 60−70 °C, a catalytic amount of 18-crown-6 was added. The mixture was heated at 60−70 °C overnight until no starting materials were detected by GC/MS. The mixture was then poured into water.

Solid was filtrated, washed with water and then methanol, and afforded crude ethyl 3-alkyl-6-bromothieno[3,2-*b*]thiophene-2-carboxylate **15a**−**e**.

Ethyl 3-alkyl-6-bromothieno[3,2-*b*]thiophene-2-carboxylate (**15a**−**e**) (0.16 mol) dissolved in LiOH (10% in water), THF, and methanol (2:6:1). The mixture was refluxed overnight until no starting materials were detected by TLC. THF was evaporated, and the residue was acidified with 6N HCl to afford 3-alkyl-thieno[3,2-*b*]thiophene-2-carboxylic acid **16a**−**e**.

*1-(3,4-Dibromothiophen-2-yl)ethanone (**14a**).* Crude yields: 95% mp 75−78 °C. ^{1}H NMR (300 MHz, CD_2Cl_2): δ 7.67 (s, 1H), 2.69 (s, 3H). ^{13}C NMR (75 MHz, CD_2Cl_2): 189.6, 140.6, 130.2, 118.0, 117.3, 29.7. HRMS (EI) for $C_6H_4Br_2OS$: calcd, 281.83 found, 280.97 [M − H] and 282.91 [M − H + 2]. The dual molecular ion species are characteristic of a single bromide due to the presence of two isotopes of bromide.

*Ethyl 6-Bromo-3-methylthieno[3,2-b]thiophene-2-carboxylate (**15a**).* **15a** was purified with flash column chromatography. Yields: 95% mp 91−92 °C. ^{1}H NMR (300 MHz, CD_2Cl_2): δ 7.48 (s, 1H), 4.36 (q, 2H), 2.63 (s, 3H), 1.38 (t, 3H). ^{13}C NMR (75 MHz, CD_2Cl_2): 163.2, 141.7, 141.4, 138.9, 129.5, 127.9, 103.5, 61.6, 14.9. HRMS (EI) for $C_{10}H_7BrO_2S_2$: calcd, 303.92; found, 303.20 [M − H] and 305.13 [M − H + 2].

*6-Bromo-3-methylthieno[3,2-b]thiophene-2-carboxylic Acid (**16a**).* Overall yield: 86%. mp 280−282 °C. ^{1}H NMR (300 MHz, TDF): δ 7.68 (s, 1H), 2.69 (s, 3H). ^{1}H NMR (300 MHz, CD_2Cl_2): δ 7.67 (s, 1H), 2.69 (s, 3H). ^{1}H NMR (300 MHz, DMSO-d_6): δ 8.07 (s, 1H), 2.60 (s, 3H). ^{13}C NMR (75 MHz, DMSO-d_6): 163.6, 140.7, 140.1, 137.7, 129.7, 129.2, 102.1, 14.2. HRMS (EI) for $C_8H_5BrO_2S_2$: calcd, 275.89; found, 275.06 [M − H], 276.92 [M − H + 2], due to the presence of two isotopes of bromide.

*6-Bromo-3-octylthieno[3,2-b]thiophene-2-carboxylic Acid (**16b**).* Overall yield: 86%. ^{1}H NMR (300 MHz, TDF): δ 11.67 (br, 1H), 7.79 (s, 1H), 3.18 (t, 2H), 1.45−1.33 (m, 12H), 0.92 (t, 3H). HRMS (EI) for $C_{15}H_{19}BrO_2S_2$: calcd, 374.00; found, 373.07 [M − H], 375.00 [M − H + 2]

*6-Bromo-3-undecylthieno[3,2-b]thiophene-2-carboxylic Acid (**16c**).* Overall yield: 56%. ^{1}H NMR (300 MHz, TDF): δ 11.61 (br, 1H), 7.73 (s, 1H), 3.18 (t, 2H), 1.35−1.28 (m, 16H), 0.88 (t, 3H). HRMS (EI) for $C_{18}H_{25}BrO_2S_2$: calcd, 416.05; found, 415.15 [M − H], 417.01[M − H + 2].

*6-Bromo-3-tridecylthieno[3,2-b]thiophene-2-carboxylic Acid (**16d**).* Overall yield: 46%. ^{1}H NMR (300 MHz, CD_2Cl_2): δ 7.55 (s, 1H), 3.17 (t, 2H), 1.78−1.75 (t, 2H), 1.42−1.28 (m, 22H), 0.87 (t, 3H). ^{1}H NMR (300 MHz, TDF): δ 11.58 (br, 1H), 7.72 (s, 1H), 3.18 (t, 2H), 1.35−1.22 (m, 22H), 0.88 (t, 3H). HRMS (EI) for $C_{20}H_{29}BrO_2S_2$: calcd, 444.08; found, 443.09 [M − H], 445.02 [M − H + 2]

*6-Bromo-3-pentadecylthieno[3,2-b]thiophene-2-carboxylic Acid (**16e**).* Overall yield 59%. ^{1}H NMR (300 MHz, TDF): δ 11.63 (br, 1H), 7.72 (s, 1H), 3.18 (t, 2H), 1.35−1.22 (m, 25H), 0.88 (t, 4H). HRMS (EI) for $C_{22}H_{33}BrO_2S_2$: calcd, 472.11; found, 471.27 [M − H], 473.13 [M − H + 2].

Compounds and Reagents. Zaprinast was obtained from Enzo Life Sciences (Plymouth Meeting, PA). Compound **17** was obtained from Ryan Scientific, Inc. (Mt. Pleasant, SC). Epic 384-well biosensor microplates were obtained from Corning Inc. (Corning, NY, USA).

Cell Culture. Human colorectal adenocarcinoma HT-29 was obtained from American Type Cell Culture (Manassas, VA, USA). The cells were cultured in McCoy's 5a Medium Modified supplemented with 10% fetal bovine serum, 4.5 g/L glucose, 2 mM glutamine, and antibiotics at 37 °C under air/5% CO_2. Tango GPR35-bla U2OS cells were purchased from Invitrogen. The cells were cultured according to the protocols recommended by the supplier. Briefly, the cells were passed using McCoy's 5A medium (Invitrogen 16600−082) supplemented with 10% dialyzed fetal bovine serum, 0.1 μM NEAA, 25 μM Hepes (pH 7.3), 1 mM sodium pyruvate, 100 U/mL penicillin, 100 μg/mL streptomycin, 200 μg/mL zeocin, 50 μg/mL hygromycin, and 100 μg/mL geneticin in a humidified 37 °C/5% CO_2 incubator.

DMR Assays Using Epic System. All DMR assays were performed using Epic system (Corning Inc., Corning, NY). Epic is a wavelength interrogation reader system tailored for resonant waveguide grating biosensors in microtiter plates. This system consists of a temperature-control unit (26 °C), an optical detection unit, and an on-board liquid handling unit with robotics. The detection unit is centered on integrated fiber optics and enables kinetic measures of cellular responses with a time interval of ∼15 s. Cells were directly seeded in Epic plates and cultured overnight to form a confluent monolayer in the cell culture medium. After being washed twice, the cells were maintained with Hank's Balanced Salt Solution and further incubated inside the system for 1 h. For agonist screen, a 2 min baseline was then established. Immediately after the compound addition using the onboard liquid handler, the cellular responses were recorded. For desensitization assays, cells were initially treated with compounds for 1 h, followed by stimulation with zaprinast at a fixed dose. The cellular responses were recorded throughout the assays. All EC_{50} or IC_{50} described in the main text were calculated based on the amplitudes of DMR signals at 8 min post agonist stimulation. Because all GPR35 agonists led to a sustained positive-DMR (P-DMR) signal, the amplitudes at 50 min post stimulation were also used to determine kinetics dependent potency and efficacy of all ligands.

For the RNAi knockdown of GPR35, HT29 cells were seeded on Epic plates at 5000 cells/well and allowed to incubate at 37 °C for 24 h (day 1). On day 2, cells were washed with fresh growth media of HT29 once, then leave cells with 30 μL/well of growth media (McCoy's 5a media, 10× PBS, 1× Pen/Strap, all from Invitrogen, San Diego, CA, USA). Short hairpin RNA (shRNA) constructs for targeting human GPR35 mRNA were obtained from Origene (Rockville, MD, USA) and are in pGFP-V-RS vector which express green fluorescent protein (GFP) for easy determination of transfection efficiency. Transient transfection of shRNA plasmids and control plasmids was performed using Effectene transfection system from Qiagen according to manufacturer's instructions (Qiagen, Valencia, CA, USA). Briefly, 0.05 μg of plasmid DNA were mixed with Enhancer and Buffer EC for 20 min at room temperature followed by the addition of diluted Effectene solution. The final mixture were incubated at room temperature for 30 min before being dispensed to each 384-well for 20 μL/well. The Epic plates containing HT29 cells and shRNA constructs in transfection reagents were centrifuged at 500 rpm for 1 min and put back in 37 °C for incubation. On day 3, media of HT29 cells were replaced with fresh growth media at 40 μL/well and cells were allowed to incubate for another 24 h. On day 4, about 48 h post-transfection, HT29 cells were subjected to DMR assays in agonist mode as described above. Zaprinast was obtained from Tocris Chemical Co. (St. Louis, MO, USA). All compounds were stocked in DMSO at 10 mM and were diluted directly in the assay buffer (1× Hanks' Balanced Salt Buffer, 20 mM Hepes, pH 7.1; HBSS) to the indicated concentrations. Epic 384-well biosensor microplates were obtained from Corning Inc.

Receptor Internalization Assays. HT29 cells were plated on an 8-well chamber slide (Nalge Nunc International, Rochester, NY, USA) with a seeding density of 10000 cells per well and incubated at 37 °C for 24 h. Next day, cells were stimulated with a compound or equal amount of DMSO at 37 °C for 1 h. Afterward, cells were fixed with 4% formaldehyde in 1× PBS for 15 min, followed by blocking and permeabilization in a buffer containing 4% goat serum, 0.1% bovine serum albumin (BSA), 0.1% Triton X100 in 1× PBS for 2 h. After 5 min wash with PBS, fixed cells were incubated with the anti-GPR35 (1:500) (anti-GPR35, T-14, intracellular domain) (Santa Cruz Biotechnology, Santa Cruz, CA, USA) in 3% BSA/PBS buffer for 24 h, followed by incubation with secondary antibody Alexa Fluor 594 donkey antigoat IgG (H + L) (1:500) (Invitrogen) in 3% BSA/PBS for 1 h at room temperature. Cells were finally washed once with PBS and sealed with 1.5 mm thick glass coverslip (Corning, NY). Dried slides were stored at 4 °C until imaging. Confocal imaging was performed with Zeiss confocal microscope Axiovert 40. The collected images were analyzed using MacBiophotonics Image J software (http://www.macbiophotonics.ca/downloads.htm).

Western Blotting. Transfection of shRNA constructs were performed in 6-well tissue culture treated plate (Corning) with Effectene transfection system according to manufacturer's instructions (Qiagen). Two days following transfection, cells were washed with PBS once and lysed with NP40 lysis buffer (Invitrogen) containing 1× protease inhibitor cocktail (Fisher Scientific) and the whole cell lysate was harvested and centrifuged at 20000 rpm for 20 min at 4 °C. Supernatant (cytoplasmic fraction) of the cell lysate was collected and subjected to BCA assay (Sigma Aldrich, St. Louis, MO, USA) to determine the protein concentration. Then 100 μg of cytoplasmic fraction of cell lysates were subjected to electrophoresis in 10× Nu-PAGE gel (Invitrogen), followed by being transferred to HyBond PDVF membrane (GE Healthcare Life Science, Piscataway, NJ, USA). For blotting, the protein membrane was blocked with 5% milk in TBST (0.05% Tween) and then incubated with anti-GPR35 (1:500) (Santa Cruz) for overnight at 4 °C. Next day, the membrane was washed with PBS for 3 times with 10 min each and incubated with antirabbit IgG conjugated horseradish peroxidase for 1 h at room temperature, followed by enhanced chemiluminescence detection with ECL plus (GE Healthcare Life Science). Equivalent gel loading was confirmed by probing with β-actin antibody (Santa Cruz).

Tango β-Arrestin Translocation Gene Reporter Assays. Tango GPR35-*bla* U2OS cells was used. This cell line stably expresses two fusion proteins: human GPR35 linked to a TEV protease site and a Gal4-VP16 transcription factor and β-arrestin/TEV protease fusion protein. The cell line also stably expresses the β-lactamase reporter gene under the control of a UAS response element. The activation of GPR35 by agonists leads to the recruitment of β-arrestin/TEV protease fusion proteins to the activated GPR35. As a result, the protease cleaves the Gal4-VP16 transcription factor from the receptor, which then translocates to the nucleus and activates the expression of β-lactamase. Briefly, 10000 cells per well were seeded in 384-well, black-wall, clear-bottom assay plates with low fluorescence background (Corning) and cultured in Dulbecco's Modified Eagle Medium (Invitrogen, 10569−010) supplemented with 10% dialyzed fetal bovine serum, 0.1 μM nonessential amino acids, 25 μM Hepes (pH 7.3), 100 U/mL penicillin, and 100 μg/mL streptomycin. After overnight culture, the cells were stimulated with ligands for 5 h in a humidified 37 °C/5% CO_2 and then loaded with the cell permeable LiveBLAzer FRET B/G substrate. After the 2 h incubation, the coumarin:fluorescein ratio was measured using Tecan Safire II microplate reader (Männedorf, Switzerland). In the absence of β-lactamase expression (i.e., no GPR35 activation), cells generated green fluorescence. In the presence of β-lactamase expression upon receptor activation, the substrate was cleaved and the cells generated blue fluorescence. The coumarin:fluorescein ratio was used as a normalized reporter response.

■ ASSOCIATED CONTENT

Supporting Information. Characterization of compounds **10**, **11**, **12**, **13**, **15a**, **16a** (YE210), **16b**, **16c**, **16d**, and **16e**, respectively, using NMR and mass spectroscopy. This material is available free of charge via the Internet at http://pubs.acs.org.

■ AUTHOR INFORMATION

Corresponding Author
*Phone: +1-607-9747203. E-mail: fangy2@corning.com.

■ ABBREVIATIONS USED

GPR35, G protein-coupled receptor 35; GPCR, G protein-coupled receptor; NPPB, 5-nitro-2-(3-phenylpropylamino)-benzoate; DMR, dynamic mass redistribution; RNAi, interference RNA; shRNA, short hairpin RNA; FRET, fluorescence resonance energy transfer; GC/MS, gas chromatography−mass spectroscopy; TLC, thin-layer chromatography; MALDI, matrix-assisted laser deposition ionization; EI, electron ionization; HRMS, high-resolution mass spectra; GFP, green fluorescent protein

■ REFERENCES

(1) Min, K. D.; Asakura, M.; Liao, Y.; Nakamaru, K.; Okazaki, H.; Takahashi, T.; Fujimoto, K.; Ito, S.; Takahashi, A.; Asanuma, H.; Yamazaki, S.; Minamino, T.; Sanada, S.; Seguchi, O.; Nakano, A.; Ando, Y.; Otsuka, T.; Furukawa, H.; Isomura, T.; Takashima, S.; Mochizuki, N.; Kitakaze, M. Identification of genes related to heart failure using global gene expression profiling of human failing myocardium. *Biochem. Biophys. Res. Commun.* **2010**, *393*, 55–60.

(2) Sun, Y. V.; Bielak, L. F.; Peyser, P. A.; Turner, S. T.; Sheedy, P. F.; Boerwinkle, E.; Kardia, S. L. Application of machine learning algorithms to predict coronary artery calcification with a sibship-based design. *Genet. Epidemiol.* **2008**, *32*, 350–360.

(3) Yang, Y.; Lu, J. Y. L.; Wu, X.; Summer, S.; Whoriskey, J.; Saris, C.; Reagan, J. D. G-Protein-coupled receptor 35 is a target of the asthma drugs cromolyn disodium and nedocromil sodium. *Pharmacology* **2010**, *86*, 1–5.

(4) Zhao, P.; Sharir, H.; Kapur, A.; Cowan, A.; Geller, E. B.; Adler, M. W.; Seltzman, H. H.; Reggio, P. H.; Heynen-Genel, S.; Sauer, M.; Chung, T. D. Y.; Bai, Y.; Chen, W.; Caron, M. G.; Barak, L. S.; Abood, M. E. Targeting of the orphan receptor GPR35 by pamoic acid: a potent activator of ERK and β-arrestin2, with antinociceptive activity. *Mol. Pharmacol.* **2010**, *78*, 560–568.

(5) Cosi, C.; Mannaioni, G.; Cozzi, A.; Carlà, V.; Sili, M.; Cavone, L.; Maratea, D.; Moroni, F. G-Protein coupled receptor 35 (GPR35) activation and inflammatory pain: studies on the antinociceptive effects of kynurenic acid and zaprinast. *Neuropharmacology* **2010**, *60*, 1227–1231.

(6) Imielinski, M.; et al. Common variants at five new loci associated with early-onset inflammatory bowel disease. *Nature Genet.* **2009**, *41*, 1335–1340.

(7) Okumura, S.; Baba, H.; Kumada, T.; Nanmoku, K.; Nakajima, H.; Nakane, Y.; Hioki, K.; Ikenaka, K. Cloning of a G-protein-coupled receptor that shows an activity to transform NIH3T3 cells and is expressed in gastric cancer cells. *Cancer Sci.* **2004**, *95*, 131–135.

(8) Wang, J.; Simonavicius, N.; Wu, X.; Swaminath, G.; Reagan, J.; Tian, H.; Ling, L. Kynurenic acid as a ligand for orphan G protein-coupled receptor GPR35. *J. Biol. Chem.* **2006**, *281*, 22021–22028.

(9) Oka, S.; Ota, R.; Shima, M.; Yamashita, A.; Sugiura, T. GPR35 is a novel lysophosphatidic acid receptor. *Biochem. Biophys. Res. Commun.* **2010**, *395*, 232–237.

(10) Taniguchia, Y.; Tonai-Kachia, H.; Shinjo, K. Zaprinast, a well-known cyclic guanosine monophosphate-specific phosphodiesterase inhibitor, is an agonist for GPR35. *FEBS Lett.* **2006**, *580*, 5003–5008.

(11) Taniguchi, Y.; Tonai-Kachi, H.; Shinjo, K. 5-Nitro-2-(3-phenylpropylamino)benzoic acid is a GPR35 agonist. *Pharmacology* **2008**, *82*, 245–249.

(12) Jenkins, L.; Brea, J.; Smith, N. J.; Hudson, B. D.; Reilly, G.; Bryant, N. J.; Castro, M.; Loza, M. I.; Milligan, G. Identification of novel species-selective agonists of the G-protein-coupled receptor GPR35 that promote recruitment of β-arrestin-2 and activate $G_{\alpha 13}$. *Biochem. J.* **2010**, *432*, 451–459.

(13) Fang, Y.; Ferrie, A. M.; Li, G. Probing cytoskeleton modulation by optical biosensors. *FEBS Lett.* **2005**, *579*, 4175–4180.

(14) Fang, Y.; Ferrie, A. M.; Fontaine, N. H.; Yuen, P. K. Characteristics of dynamic mass redistribution of EGF receptor signaling in living cells measured with label free optical biosensors. *Anal. Chem.* **2005**, *77*, 5720–5725.

(15) Kenakin, T. Cellular assays as portals to seven-transmembrane receptor-based drug discovery. *Nature Rev. Drug Discovery.* **2009**, *8*, 617–626.

(16) Fang, Y. Label-free receptor assays. *Drug Discovery Today: Technol.* **2010**, *7*, e5–e11.

(17) Schröder, R.; Janssen, N.; Schmidt, J.; Kebig, A.; Merten, N.; Hennen, S.; Müller, A.; Blättermann, S.; Mohr-Andrä, M.; Zahn, S.; Wenzel, J.; Smith, N. J.; Gomeza, J.; Drewke, C.; Milligan, G.; Mohr, K.; Kostenis, E. Deconvolution of complex G protein-coupled receptor signaling in live cells using dynamic mass redistribution measurements. *Nature Biotechnol.* **2010**, *28*, 943–949.

(18) Fang, Y.; Ferrie, A. M.; Fontaine, N. H.; Mauro, J.; Balakrishnan, J. Resonant waveguide grating biosensor for living cell sensing. *Biophys. J.* **2006**, *91*, 1925–1940.

(19) Fang, Y. Probing cancer signaling with resonant waveguide grating biosensors. *Exp. Opin. Drug Discovery* **2010**, *5*, 1237–1248.

(20) He, M.; Leslie, T. M.; Sinicropi, J. A. α-Hydroxy ketone precursors leading to a novel class of electro-optic acceptors. *Chem. Mater.* **2002**, *14*, 2393–2400.

(21) He, M.; Zhang, F. Synthesis and structure of alkyl-substitute fused thiophenes containing up to seven rings. *J. Org. Chem.* **2007**, *72*, 2542–2544.

(22) Deng, H.; Hu, H.; Fang, Y. Tyrphostin analogs are GPR35 agonists. *FEBS Lett.* **2011**, *585*, 1957–1962.

(23) Fang, Y.; Ferrie, A. M. Optical biosensor differentiates signaling of endogenous PAR_1 and PAR_2 in A431 cells. *BMC Cell Biol.* **2007**, *8*, 24.

(24) Charlton, S. J. Agonist efficacy and receptor desensitization: from partial truths to a fuller picture. *Br. J. Pharmacol.* **2009**, *158*, 165–168.

(25) Goral, V.; Jin, Y.; Sun, H.; Ferrie, A. M.; Wu, Q.; Fang, Y. Agonist-directed desensitization of the β_2-adrenergic receptor. *PLoS One* **2011**, *6*, e19282.

(26) Fang, Y.; Deng, H.; Ferrie, A. M.; He, M.; Hu, H.; Niu, W. Compositions and methods for the treatment of pathological condition-(s) related to GPR35. US Patent Application 13/182019, 2010.

(27) Mailmana, R. B. GPCR functional selectivity has therapeutic impact. *Trends Pharmacol. Sci.* **2007**, *8*, 390–396.